About Teaching General Relativity: history, motivation, experiment

AAPT Topical Workshop on Teaching General Relativity to Undergraduates

Rainer Weiss, MIT

Syracuse University

July 21, 2006

Outline

- Credentials ?
- Why not Lorentz covariant scalar theory: Nordstrom
- How to motivate curved geometry: rotating platform
- Should one have believed the three famous tests
  - Red shift before Pound/Rebka
  - Bending of Light before quasars
  - Perihelion advance before Hulse/Taylor
- Slippery idea of coordinate freedom : Shapiro test
- Einstein got caught too :1916 vs 1918 papers
- Bright future: GR now part of science

Lorentz Covariant Theories of Gravitation

"General Relativity and Lorentz-Invariant Theories of Gravitation " G.J. Whitrow G.E. Murdoch Nature **188** 790 (1960)
" Brief Review of Lorentz-Covariant Scalar Theories of Gravitation" A.L. Harvey American Journal of Physics 33 449 (1965)

Nordstrom Scalar Theory

Nordstrom Annalen der Physik **40** 877 1913
Nordstrom Annalen der Physik **42** 533 1913
Nordstrom Annalen der Physik **43** 1101 1914
Von Laue Jahrbuch der Radioactivitat und Electronik **14** 263 1917

Source equation: $\Box\varphi = -\frac{G(\varphi)}{c^2}T_{ii}$

"Newtonian G" coupling depends on φ : $G(\varphi) = \frac{G_0}{\left(1 + \frac{G_0}{c^2}(\varphi - \varphi_0)\right)}$

Equations of motion: $\frac{d(m_{\text{inertial}}u_i)}{d\tau} = -G(\varphi)m_{\text{grav}}\nabla_i\varphi$

Gravitational energy flux : $S_i = -\frac{\delta\varphi}{\delta t}\nabla_i\varphi$ how to put scalar field energy into T_{ii} ?

theory	perihelion	deflection	red shift	accl of cm	geodetic prec	Lense Thirring
GR	1	1	1	0	1	1
Nordstrom	-1/3	0	1	1	0	0

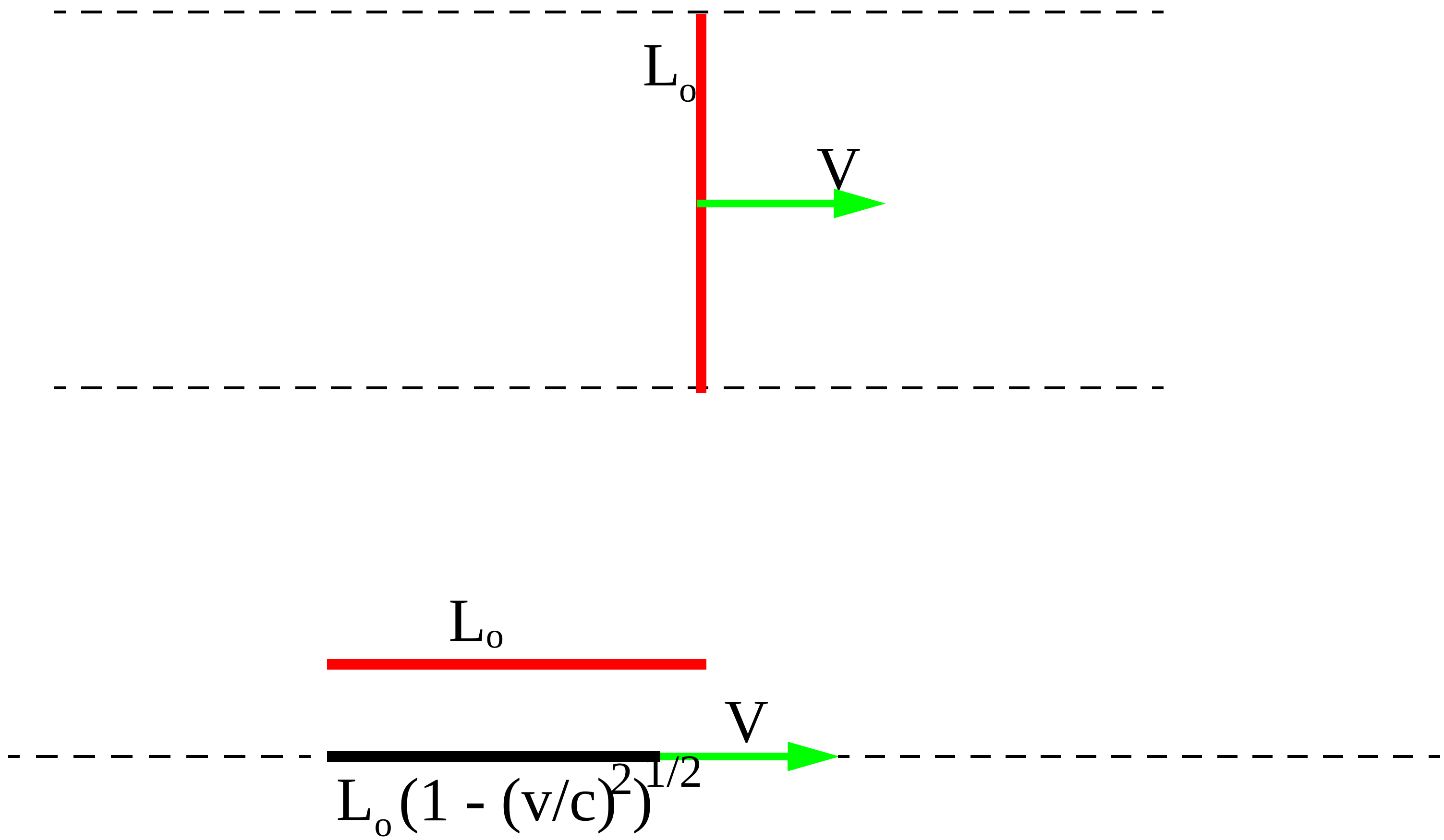

Special relativistic length contraction and simultaneous measurement

Imagining a rotating platform

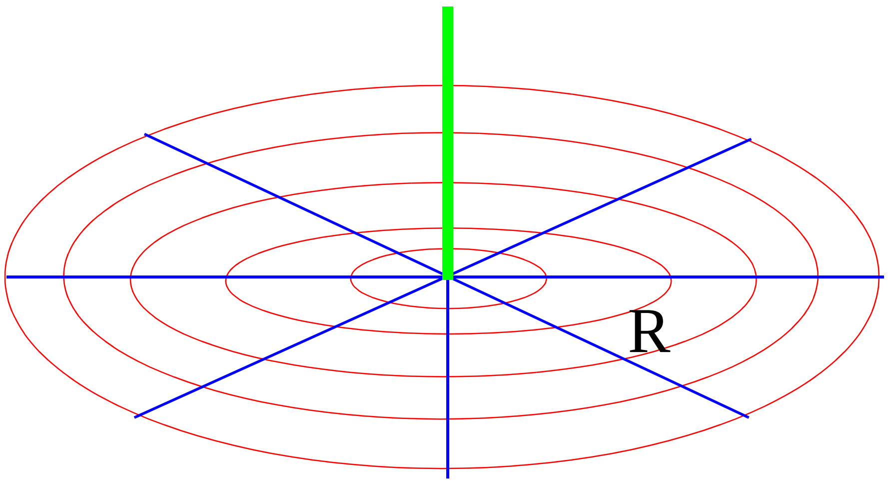

$C=2\pi R$

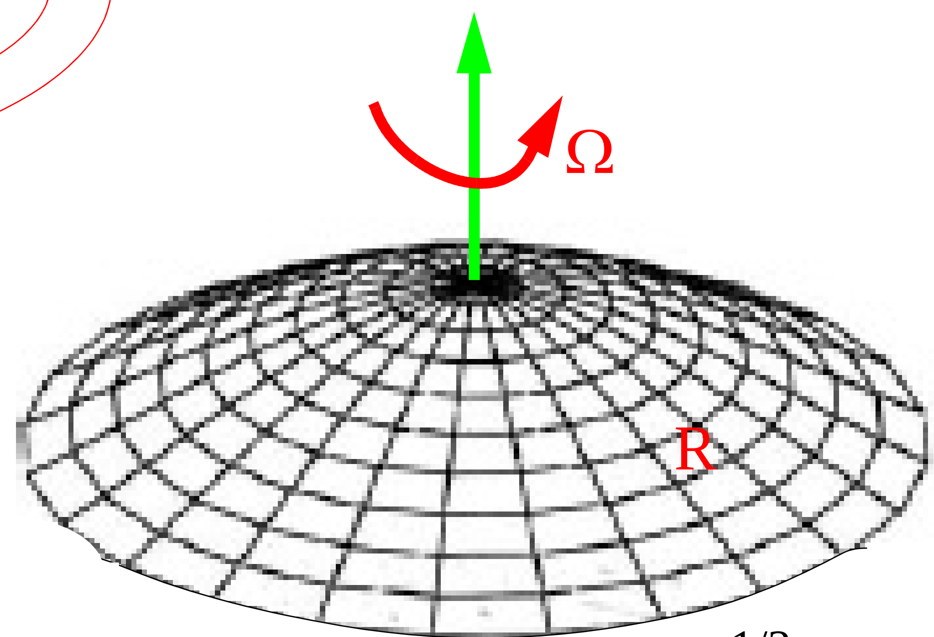

$$C = 2\pi R(1 - (\Omega R/c)^2)^{1/2}$$

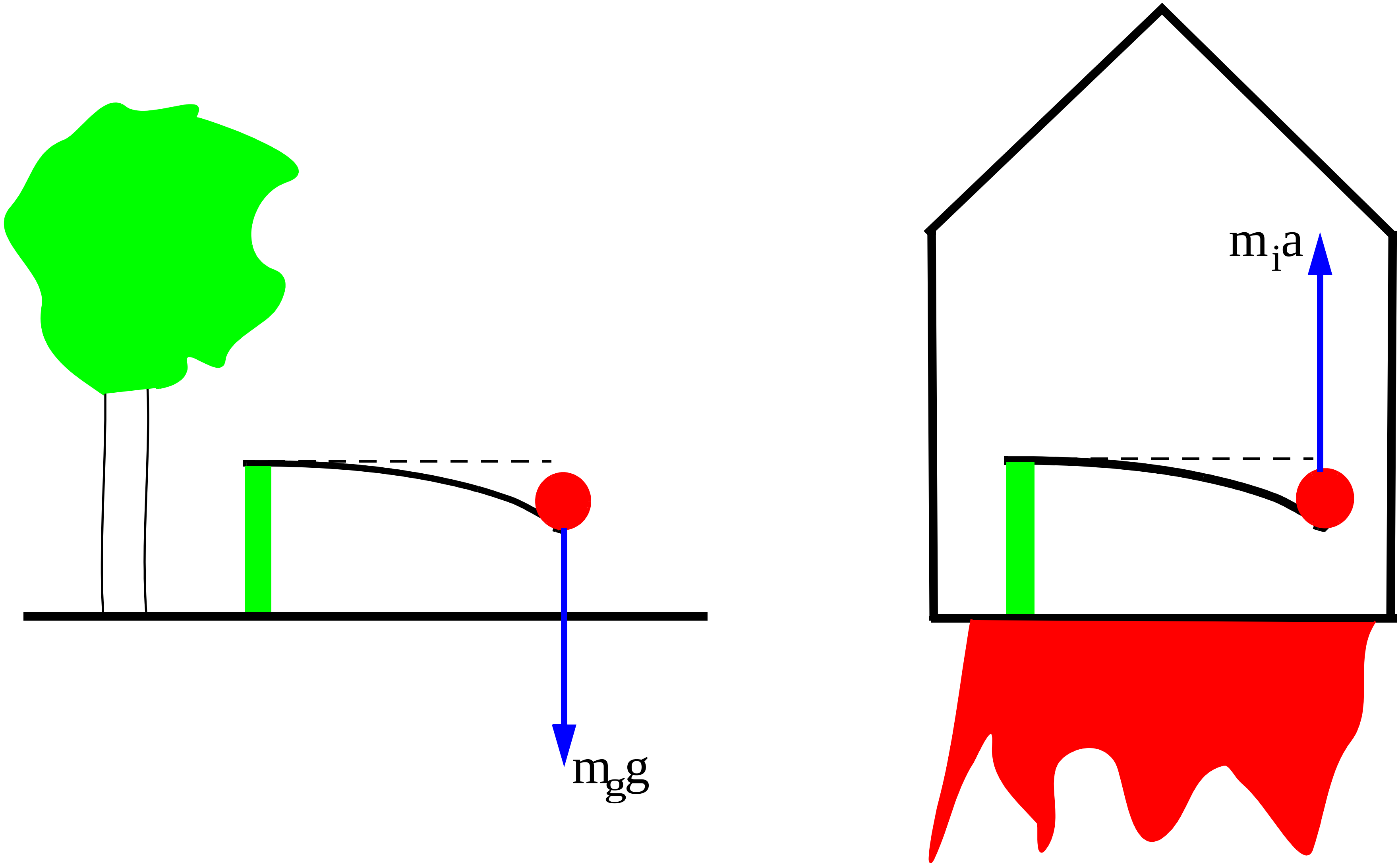

Principle of Equivalence

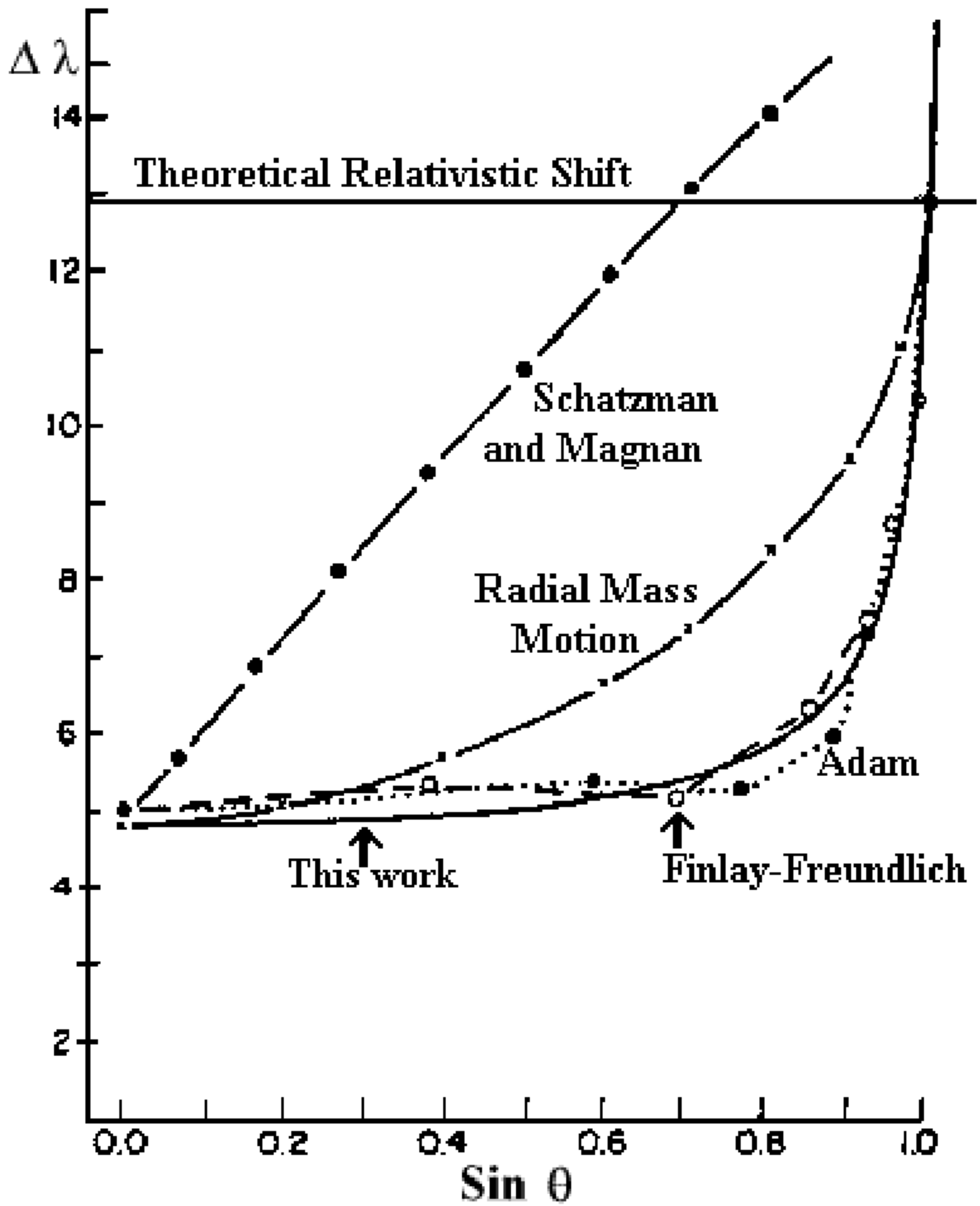

Δλ
14
Theoretical Relativistic Shift
12
10
Schatzman and Magnan
8
Radial Mass Motion
6
Adam
4
This work
Finlay-Freundlich
2
0.0
0.2
0.4
0.6
0.8
1.0
Sin θ

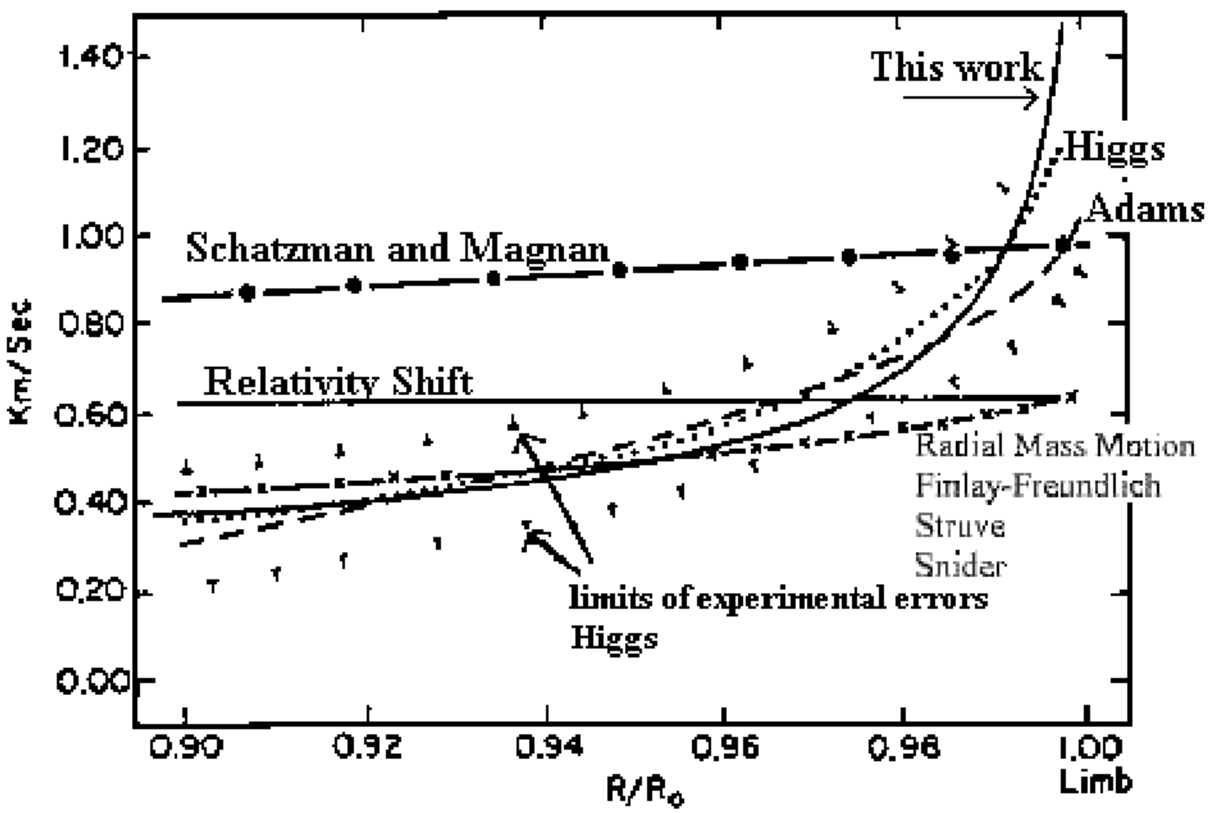

This work
Higgs
Adams
Schatzman and Magnan
Relativity Shift
Radial Mass Motion
Finlay-Freundlich
Struve
Snider
limits of experimental errors
Higgs
Km/Sec
1.40
1.20
1.00
0.80
0.60
0.40
0.20
0.00
0.90
0.92
0.94
0.96
0.96
1.00
Limb
R/R₀

CASE STUDY 1: THE DEFLECTION OF LIGHT

References:

"The Determination of Einstein's Light-Deflection in the Gravitational Field of the Sun"
H. von Klüber in *VISTAS IN ASTRONOMY* V3, 47 (1960)

"A Confirmation of Einstein's General Theory of Relativity by Measuring the Bending of Microwave Radiation in the Gravitational Field of the Sun" E.B. Fomalont and R.A. Sramek , *Astrophysical Journal* V199,749 (1975)

"Further Experimental Tests of Relativistic Gravity Using the Binary Pulsar PSR 1913 + 16"
J.H. Taylor and J. M. Weisberg, *Astrophysical Journal* V345, 434 (1989)

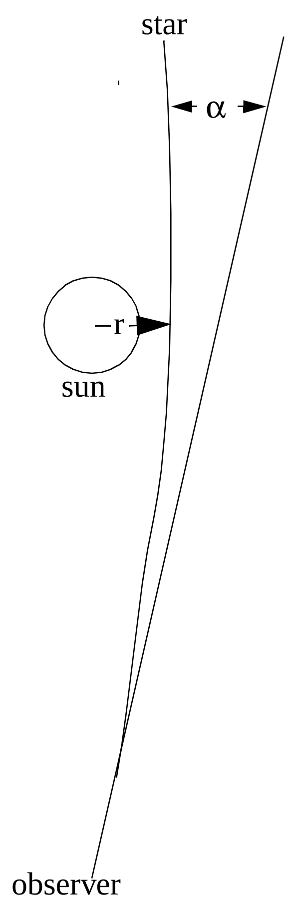

$$\alpha = \frac{4GM}{rc^2}$$

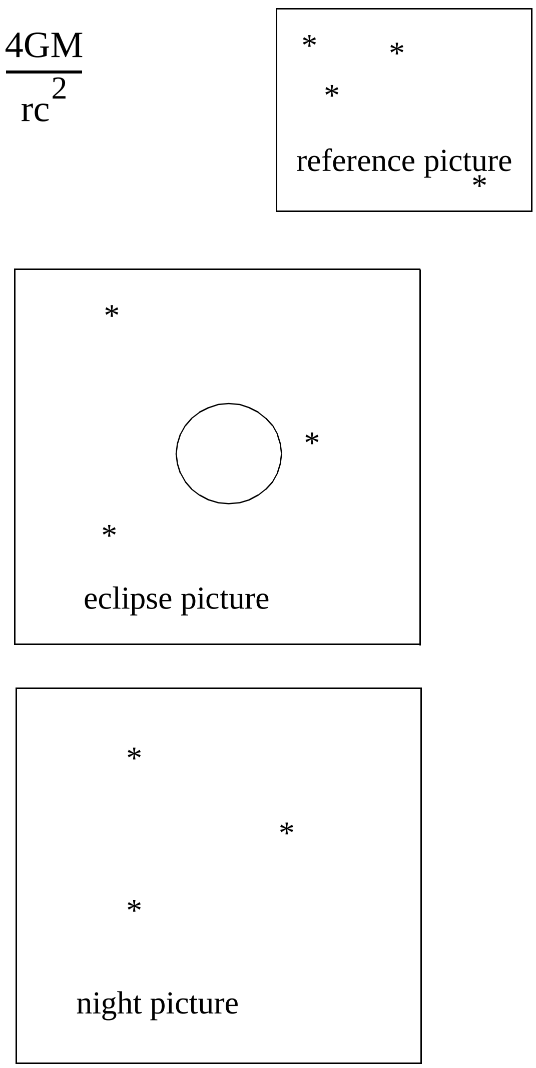

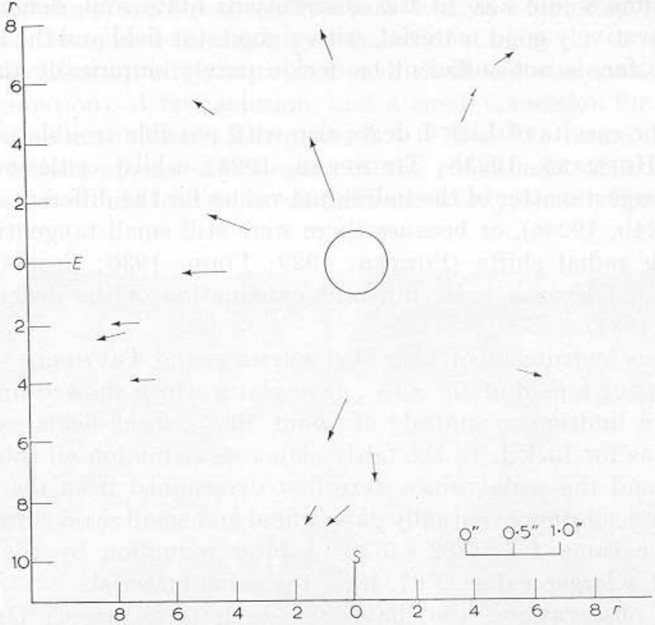

FIG. 9. Vector diagram of the radial shifts, derived from means of the 15 best stars by the Lick I and Lick II observations in 1922. It presents a very good indication of the existence of the light-deflection (CAMPBELL and TRUMPLER, 1928)

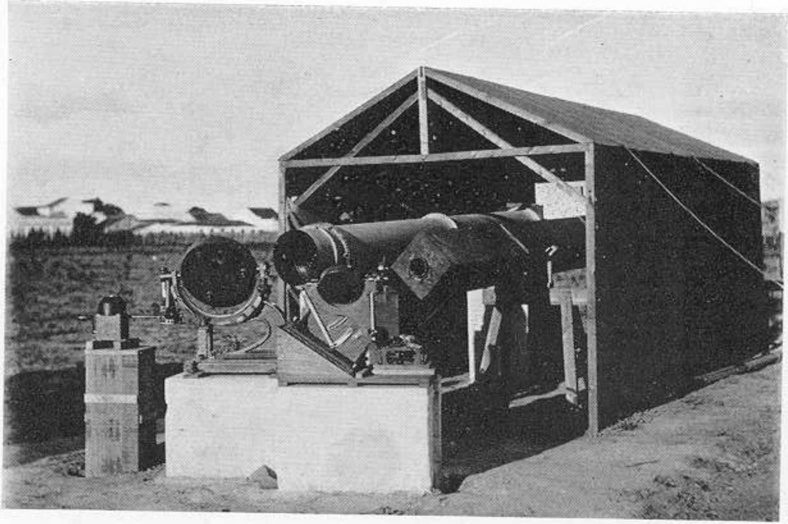

FIG. 7. The instrument used by the Greenwich expedition in 1919 at Sobral (Brazil). The two coelostats are feeding two horizontal telescopes: $f = 343$ cm and aperture 20 cm, on the left; $f = 570$ cm and 10 cm aperture, on the right; DYSON, EDDINGTON and DAVIDSON, 1920. (Photo. C. R. DAVIDSON.)

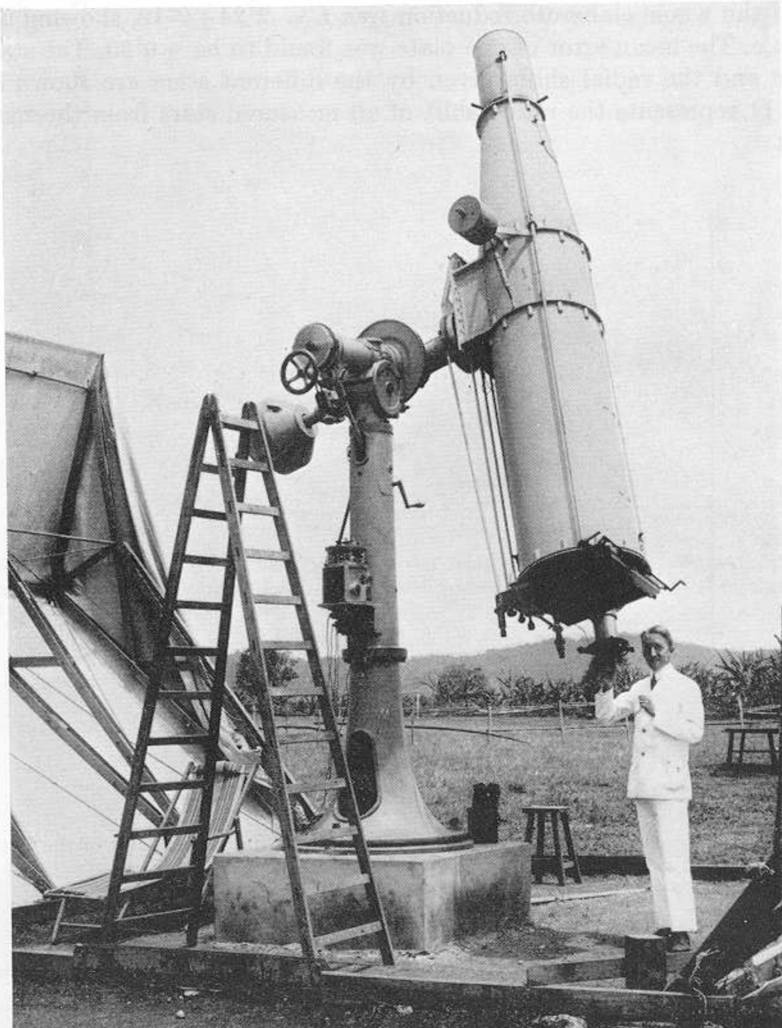

FIG. 12. Large parallactically mounted Zeiss astrograph ($f = 343$ cm, 20 cm aperture) with electrically controlled automatic drive, covering the large field of $7^{\circ}\!.5 \times 7^{\circ}\!.5$, as used in 1929 by the Potsdam observers (Potsdam II). During the eclipse itself a check star-field was photographed on each of the three plates taken of the Sun's surrounding, by pointing the astrograph alternately at a star-field distant from the Sun (FREUNDLICH, v. KLÜBER, v. BRUNN, 1933). (Photo: v. KLÜBER.)

Table 1

1	2	3	4	5	6	7	8	9	10	11	12	13	14	15	16	17	18
	Observatory (site)	Eclipse	Focal length f (cm)	Aperture ϕ (cm)	ϕ/f	Instrument (lens)	Field of plate	Number of plates	Exposure (sec)	Limiting stellar magnitude	Number of stars	r_{min} (solar radii from centre)	r_{max} (solar radii from centre)	Check-field	L	m.s.e.	Reference
1	Greenwich (Brazil)	1919 May 29	570	10	1:57	Coelostat (Double)	2°4x2°0	7	28	6(ph)	7	2	6	no	1″98	0″16	DYSON-EDDINGTON-DAVIDSON, 1920
			343	20	1:17	Coelostat (Double)	2·7×2·7	16	5–10	6(ph)	11	2	6	no	0·93	—	
2	Greenwich (Principe)	1919 May 29	343	20	1:17	Coelostat (Double)	2·7×2·7	2	2–20	6(ph)	5	2	6	no	1·61	0·40	
3	Adelaide-Greenwich (Australia)	1922 Sept. 21	160	7·5	1:21	Astrograph (Quadruple)	7×8	2	20–30	8·3	11–14	2	10	yes	1·77	0·40	DODWELL-DAVIDSON, 1924
4	Victoria (Australia)	1922 Sept. 21	330	15	1:22	Astrograph (Quadruple)	—	2	45	9·0	18	2	10	not used	1·75 1·42 2·16	—	CHANT-YOUNG, 1924.
5	Lick I (Australia)	1922 Sept. 21	450	12	1:37	Doubl. Astrograph (Double)	5×5	4	120–125	10·5(ph)	62–85	2·1	14·5	yes	1·72	0·15	CAMPBELL-TRUMPLER, 1923a.
6	Lick II (Australia)	1922 Sept. 21	150	10	1:15	Astrograph (Quadruple)	15×15	6	60–102	10·4(ph)	145	2·1	42	yes	1·82	0·20	CAMPBELL-TRUMPLER, 1928
7	Potsdam I (Sumatra)	1929 May 9	850	20	1:42	Coelostat (Double)	3×3	4	40–90	8·9	17–18	1·5	7·5	yes	2·24	0·10	FREUNDLICH-v. KLÜBER-v. BRUNN, 1931a.
8	Potsdam II (Sumatra)	1929 May 9	343	20	1:17	Astrograph (Triplet)	7·5×7·5	3	14–56	9·5	84–135	4	15	yes	—	—	FREUNDLICH-v. KLÜBER-v. BRUNN, 1933.
9	Sternberg (U.S.S.R.)	1936 June 19	600	15	1:40	Astrograph (Double)	3·5×3·5	2	25–35	9·6	16–29	2	7·2	not used	2·73	0·31	MIKHAILOV, 1949.
10	Sendai (Japan)	1936 June 19	500	20	1:25	Coelostat (Double)	2·9×2·9	2	80	8·6 (vis.)	8	4	7	no	2·13 1·28	1·15 2·67	MATUKUMA, 1940a.
11	Yerkes I (Brazil)	1947 May 20	609	15	1:40	Astrograph (Triplet)	4×4	1	185	10·2	51	3·3	10·2	not used	2·01	0·27	VAN BIESBROECK, 1949.
12	Yerkes II (Sudan)	1952 Feb. 25	609	15	1:40	Astrograph (Triplet)	4×4	2	60–90	8·6	9–11	2·1	8·6	yes	1·70	0·10	VAN BIESBROECK, 1953

Fig. 6. These 9 combined diagrams show the actually measured light-deflections for each star, as far as available, using only the data given by the authors themselves, without having regard to individual weights or group-means. Some small amendments, mainly due to scale correction, may have to be applied to the one or the other of these observational sets. The broken hyperbola represents the Einstein Effect as it should be expected from theory.

Abscissae: distances from the centre of the Sun in solar radii.

Ordinates: measured light-deflections in seconds of arc.

Inserted into the top right corners are the corresponding star fields, to a distance of about 8 solar radii from the Sun's centre. Only actually measured stars are plotted, without regard to the weight given by the observers. Co-ordinates are indicated, giving the positions of the Sun's centre for 1855·0 (B.D.-charts).

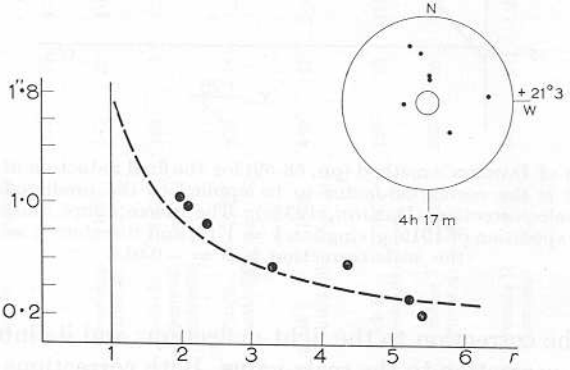

1919 Greenwich, (see Table 1, Nos. 1 and 2)

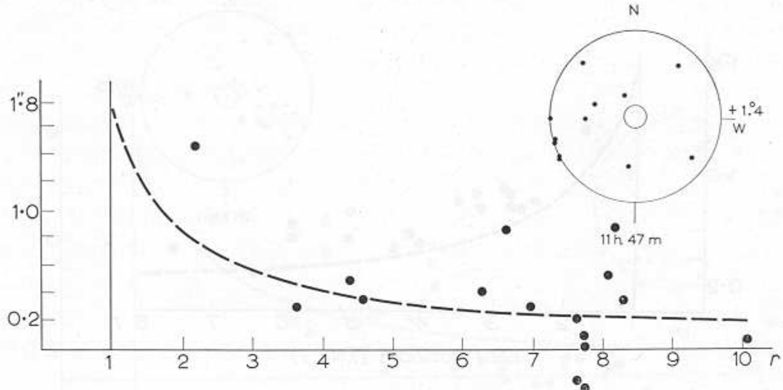

1922 Victoria (No. 4)

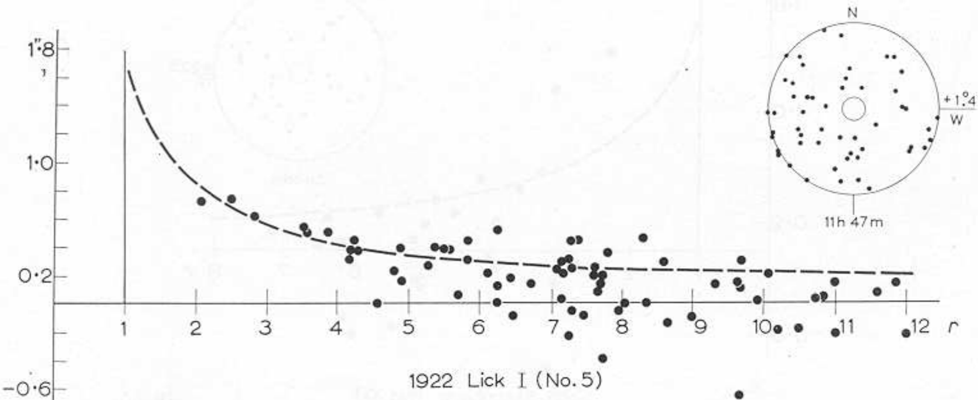

1922 Lick I (No. 5)

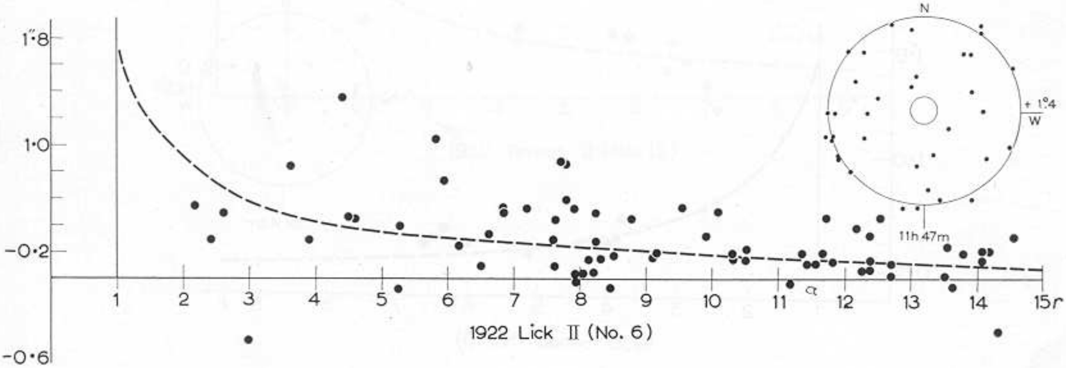

1922 Lick II (No. 6)

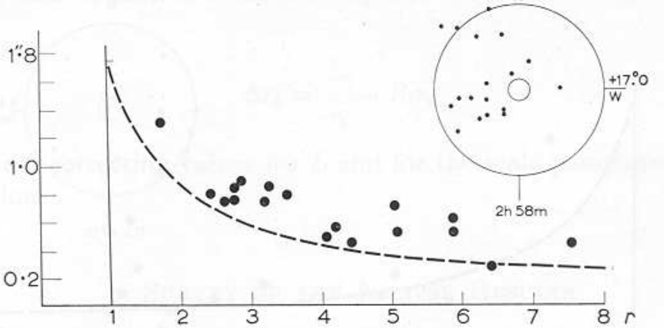

1929 Potsdam I (No 7)

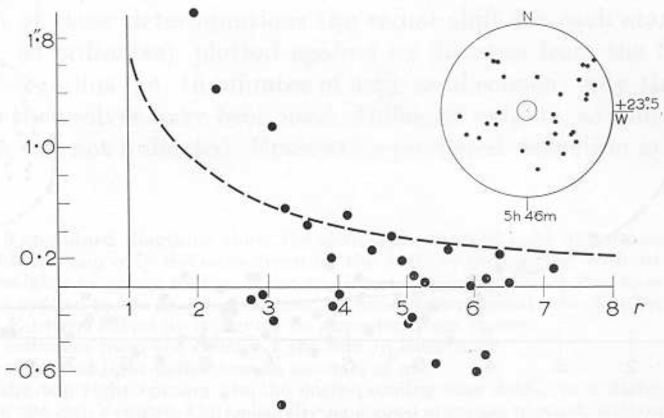

1936 Sternberg (No 9)

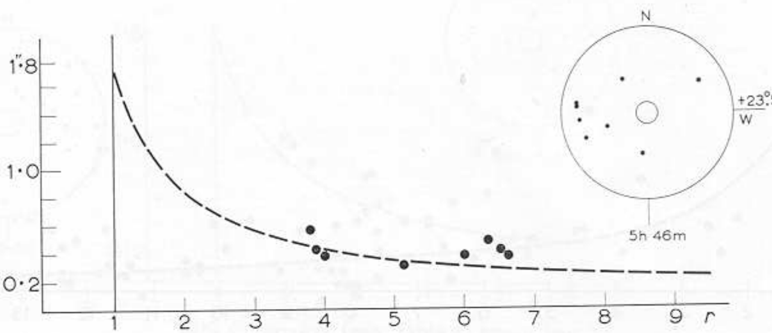

1936 Sendai (No 10)

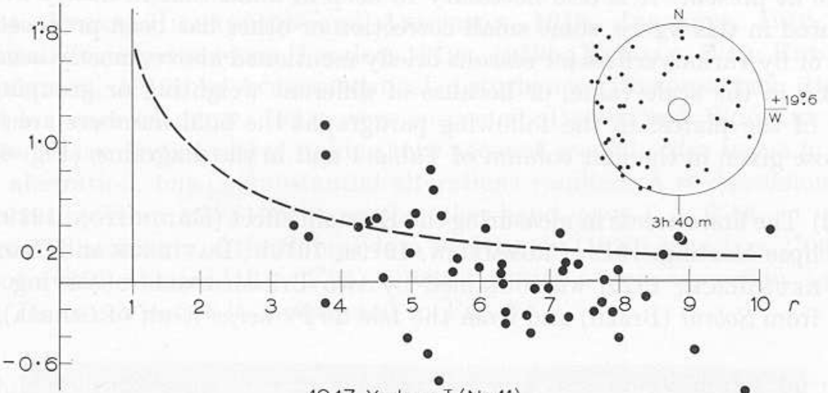

1947 Yerkes I (No 11)

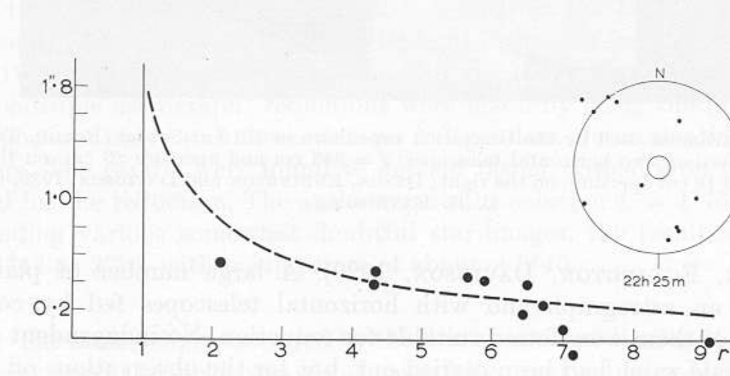

1952 Yerkes II (No. 12)

Fitting procedure for difference between stellar positions in the plates

relative translation
relative rotation
inclination of each plate relative to the telescope optic axis
scale value (magnification)
light deflection

Most significant difficulty - maintaining the scale

30% measurement @ $r = 5 \longrightarrow \Delta\alpha = 0.1\text{sec}$

$$\frac{\Delta f}{f} = \frac{\Delta L}{L} \leq 4 \times 10^{-6}$$

Inevitable thermal instabilities during the eclipse

Other difficulties

Not enough bright stars within the significant fitting region to separate scale from deflection.
Not enough observing time: 90 minutes total 1919 - 1960

BENDING BY MICROWAVE INTERFEROMETRY

$\lambda = 3.7, 11.1$ cm

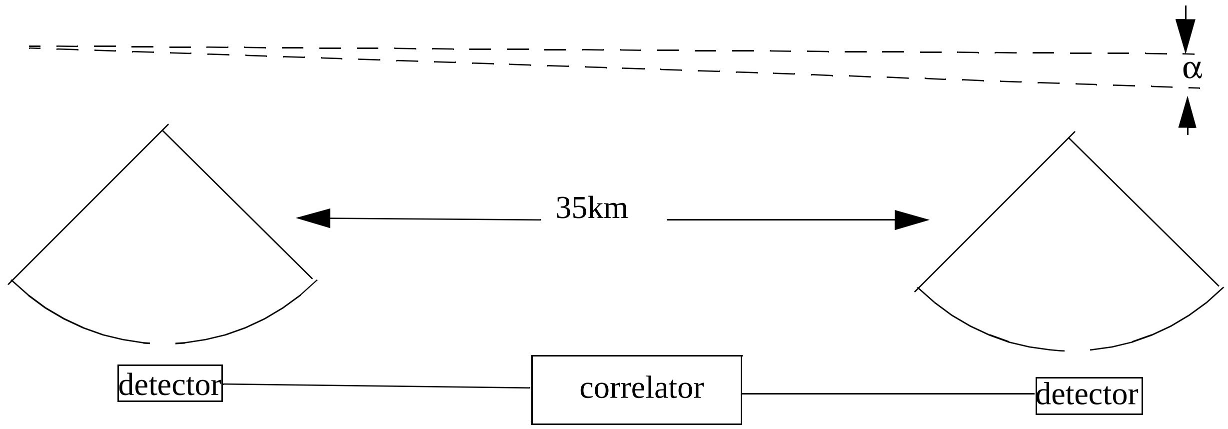

Sensitivity:

$$\Delta\alpha \approx \frac{\lambda}{L} = 1\times10^{-5} = 2 \text{seconds of arc}$$

Split fringe to 0.004 arc seconds in 8 hours of observation

Perturbations

Solar plasma: refraction varies as $\frac{1}{\omega^2}$. Separate by using two different wavelengths

Atmospheric propagation

Control

Measure relative motion of 0116+08, 0119+11 and 0111+02

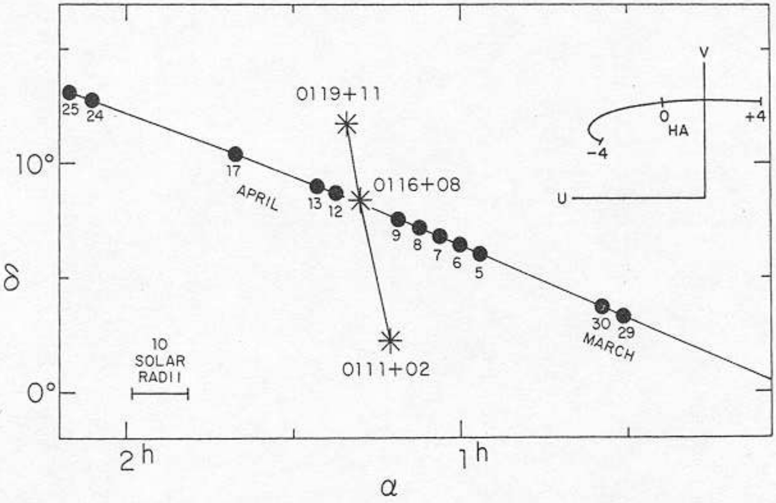

FIG. 1.—The 1974 experiment. The position of the three radio sources and the position of the Sun at noon on each observing day are shown. The coordinates refer to the epoch of date. The projected resolution of the interferometer with hour angle (HA) is given by the (u-v) plot in the upper right.

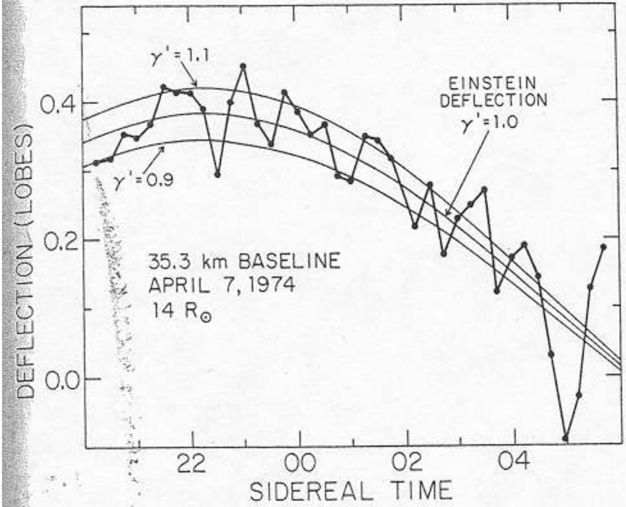

FIG. 3a

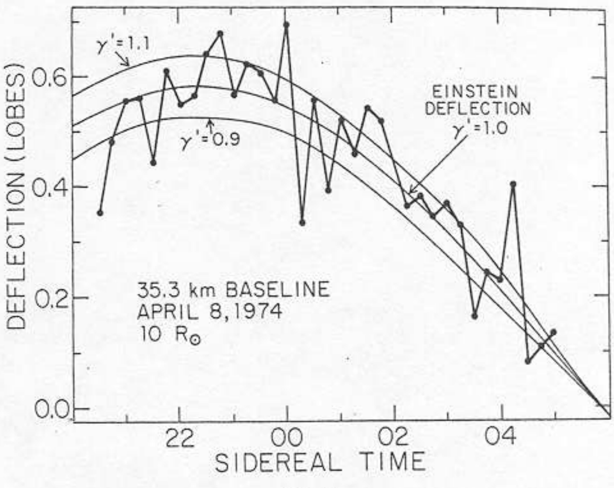

FIG. 3b

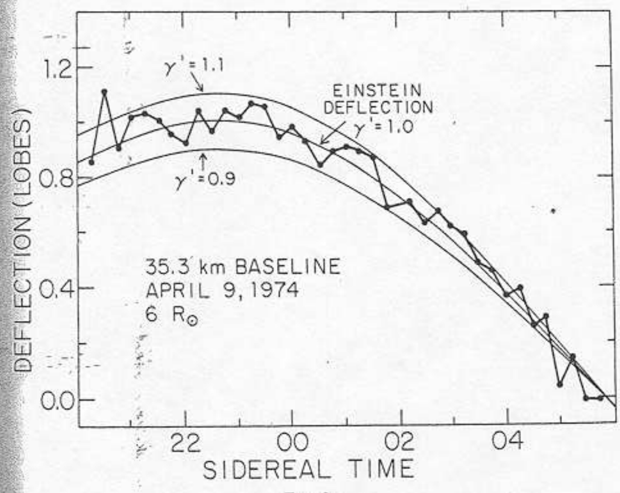

FIG. 3c

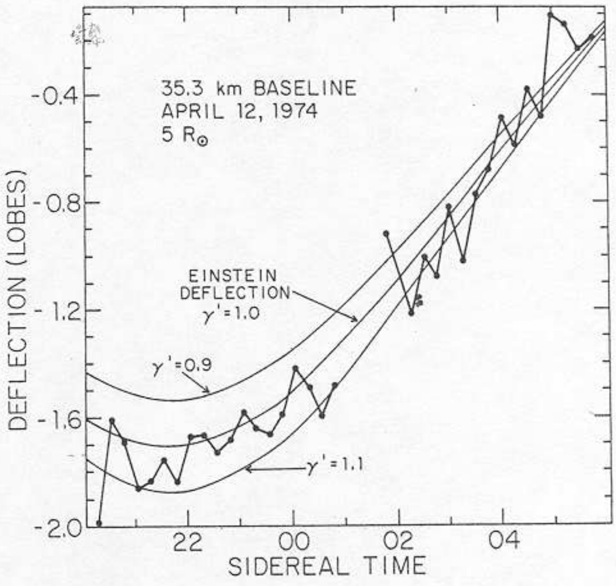

FIG. 3d

FIG. 3.—The measured corrected phase compared with the phase expected for various deflections for (*a*) April 7, (*b*) April 8, (*c*) April 9, and (*d*) April 12. All plots are for the 35.3 km baseline, left-hand polarization. The approximate distance of 0116+08 from the Sun is also given. The average phase for each determination every 15 minutes is shown by the dots.

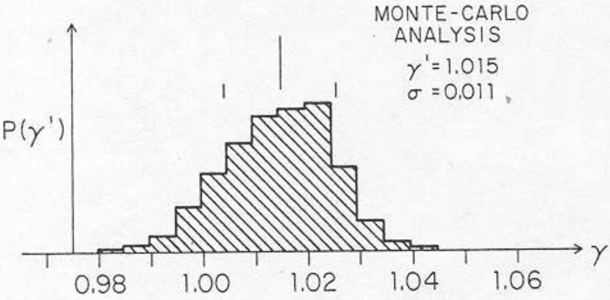

FIG. 4.—The distribution of γ', the coefficient of bending, based on a Monte Carlo analysis of the residual data. The skewness in the distribution is real and reflects the skewness of the distribution of γ' in Table 2. Only the range, not the value, of γ' was determined by this analysis.

Sources of precession of the planet Mercury as observed at the Earth
G.M. Clemence Rev Mod Phys **19** 361 1947

source	magnitude seconds arc/century
Total observed precession	5599.74 ±0.41
General precession of the equinoxes	5025.645 ±0.50
Venus	277.856 ±0.68
Earth	90.038 ±0.08
Mars	2.536 ±0.00
Jupiter	153.584 ±0.01
Saturn	7.302 ±0.01
Uranus	0.141 ±0.00
Neptune	0.042 ±0.00
Solar Oblateness (1930 German #)	0.010 ±0.02
Sum of known terms	5557.18 ±0.85
Residual	42.56 ±0.94

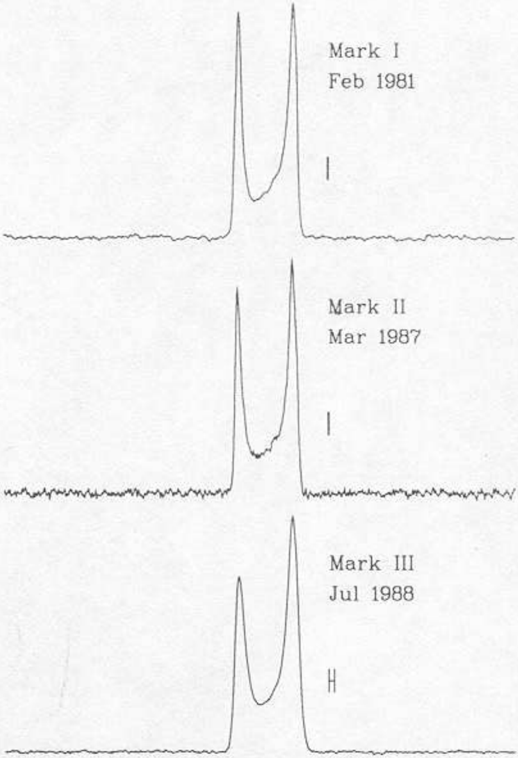

FIG. 1.—Average profiles of PSR 1913+16 as observed with the Mark I, Mark II, and Mark III data acquisition systems at frequencies near 1408 MHz. The effective time resolutions, which are dominated by dispersion smearing, are indicated by bars to the right of each pulse. The full period (59.03 ms) is plotted, and the gradual weakening of component 1 relative to component 2 is a real effect (Weisberg, Romani, and Taylor 1989).

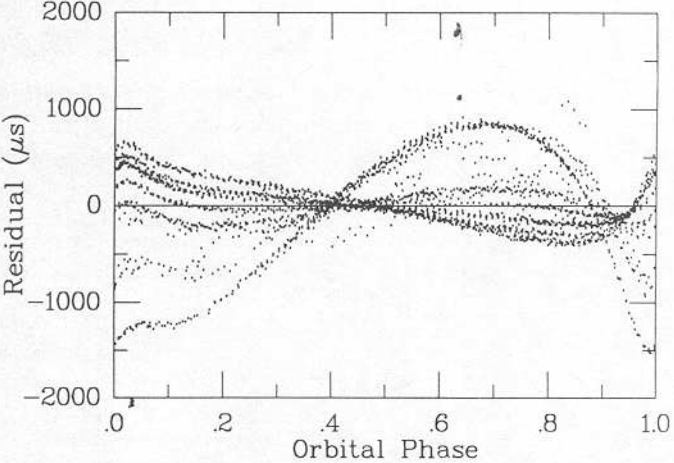

FIG. 3

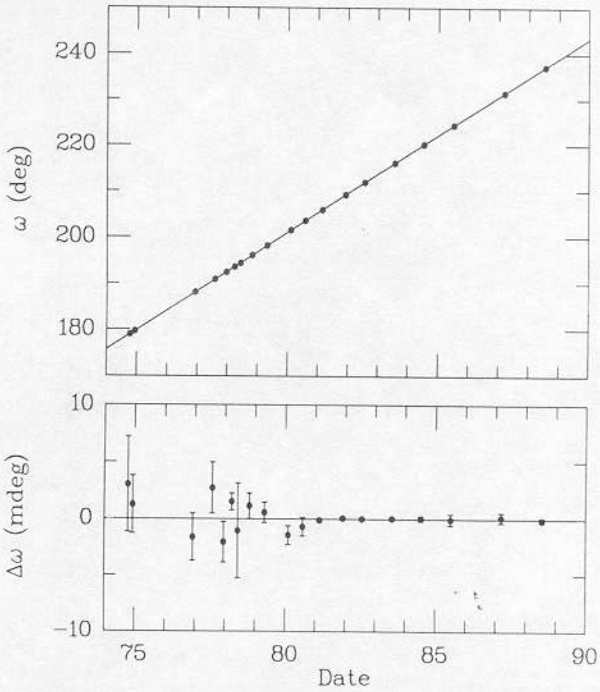

FIG. 4

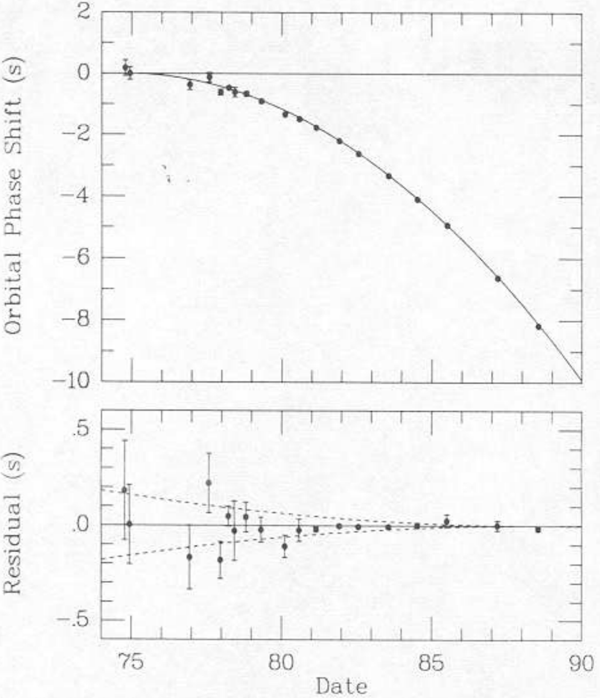

FIG. 5.—*Top:* Cumulative shift of the times of periastron passage relative to a nondissipative model in which the orbital period remains fixed at its 1974.78 value. *Bottom:* Differences between the locally measured periastron times and those expected according to the DD(1) parameter set. Dashed curves illustrate differential trends that would be expected (relative to epoch 1988.54) if the rate of orbital decay $\dot{P}_b$ were 2% larger or 2% smaller.

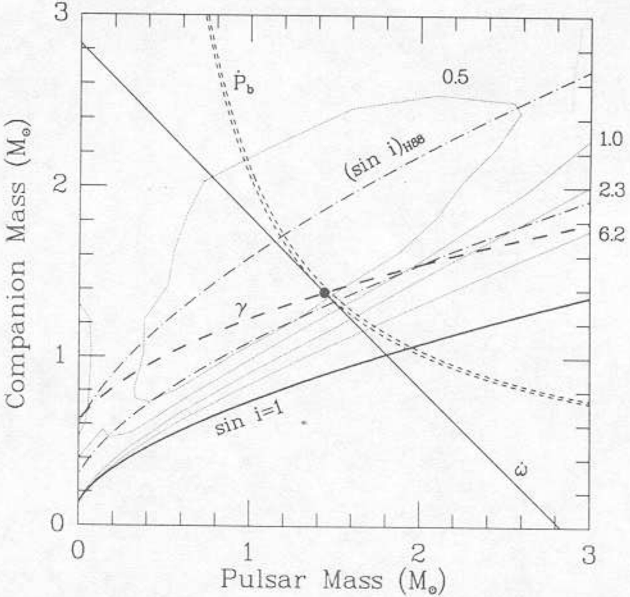

FIG. 9.—Restrictions on the pulsar mass, m_1, and companion mass, m_2, imposed by general relativity are indicated by curves labeled $\dot{\omega}$, γ, $\dot{P}_b$, and $(\sin i)_{H88}$ (the Haugan 1988 sin i parameter). Uncertainties in $\dot{\omega}$ and γ are smaller than the widths of their plotted curves; two curves are plotted for $\dot{P}_b$, and $(\sin i)_{H88}$, bracketing the uncertainty range. Numerically labeled dotted curves represent a mapping of $\Delta\chi^2$ contours for parameters r and s from Fig. 7. Companion masses below the curve labeled $\sin i = 1$ are incompatible with the mass function. The point marked with a filled circle corresponds to the mass values given for the DDGR solution in Table 5.

SHAPIRO TIME DELAY

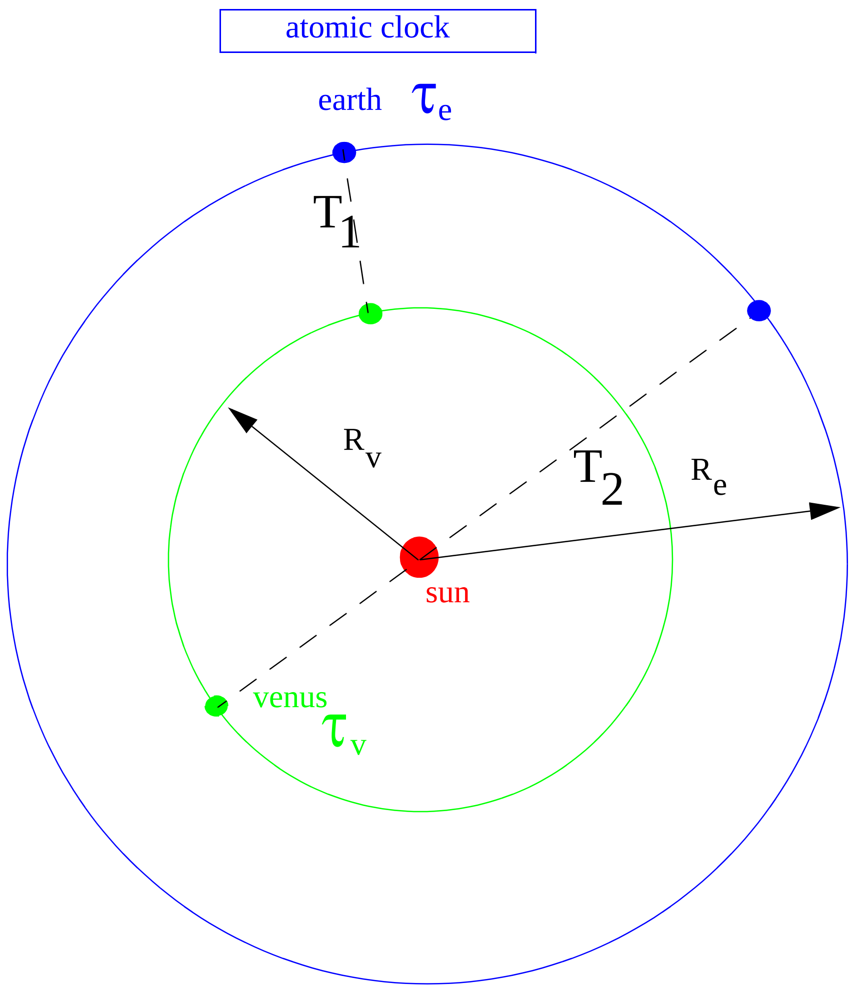

Need to make a self consistent Newtonian calculation

compare with

self consistent general relativistic one

697

SITZUNGSBERICHTE 1916.

XXXIII.

DER

KÖNIGLICH PREUSSISCHEN

AKADEMIE DER WISSENSCHAFTEN.

Näherungsweise Integration der Feldgleichungen der Gravitation.

Von A. Einstein.

$$\gamma'_{\mu\nu} = \alpha_{\mu\nu} f(x_1 + i x_4) = \alpha_{\mu\nu} f(x - t)\,. \tag{15}$$

Dabei sind die $\alpha_{\mu\nu}$ Konstante; f ist eine Funktion des Arguments $x - t$. Ist der betrachtete Raum frei von Materie, d. h. verschwinden die $T_{\mu\nu}$, so sind die Gleichungen (6) durch diesen Ansatz erfüllt. Die Gleichungen (4) liefern zwischen den $\alpha_{\mu\nu}$ die Beziehungen

$$\left.\begin{aligned} \alpha_{11} + i\alpha_{14} &= 0 \\ \alpha_{12} + i\alpha_{24} &= 0 \\ \alpha_{13} + i\alpha_{34} &= 0 \\ \alpha_{14} + i\alpha_{44} &= 0 \end{aligned}\right\}. \tag{16}$$

Von den 10 Konstanten $\alpha_{\mu\nu}$ sind daher nur 6 frei wählbar. Wir können die allgemeinste Welle der betrachteten Art daher aus Wellen von folgenden 6 Typen superponieren

$$\left.\begin{array}{lll} \text{a)}\ \begin{array}{l}\alpha_{11} + i\alpha_{14} = 0 \\ \alpha_{14} + i\alpha_{44} = 0\end{array} & \begin{array}{l}\text{b)}\ \alpha_{12} + i\alpha_{24} = 0 \\ \text{c)}\ \alpha_{13} + i\alpha_{34} = 0\end{array} & \begin{array}{l}\text{d)}\ \alpha_{22} \neq 0 \\ \text{e)}\ \alpha_{23} \neq 0 \\ \text{f)}\ \alpha_{33} \neq 0\end{array} \end{array}\right\}. \tag{17}$$

$$\begin{aligned} \text{d)}\quad \frac{1}{i} t_{22} &= \frac{f'^2}{4\varkappa}\alpha_{22}^2 = \frac{1}{4\varkappa}\left(\frac{\partial \gamma'_{22}}{\partial t}\right)^2 \\ \text{e)}\quad \frac{1}{i} t_{23} &= \frac{f'^2}{4\varkappa}\alpha_{23}^2 = \frac{1}{4\varkappa}\left(\frac{\partial \gamma'_{23}}{\partial t}\right)^2 \\ \text{f)}\quad \frac{1}{i} t_{33} &= \frac{f'^2}{4\varkappa}\alpha_{33}^2 = \frac{1}{4\varkappa}\left(\frac{\partial \gamma'_{33}}{\partial t}\right)^2 \end{aligned}$$

Es ergibt sich also, daß nur die Wellen des letzten Typs Energie transportieren, und zwar ist der Energietransport einer beliebigen ebenen Welle gegeben durch

$$I_x = \frac{1}{i} t_{41} = \frac{1}{4\varkappa}\left[\left(\frac{\partial \gamma'_{22}}{\partial t}\right)^2 + 2\left(\frac{\partial \gamma'_{23}}{\partial t}\right)^2 + \left(\frac{\partial \gamma'_{33}}{\partial t}\right)^2\right]. \tag{18}$$

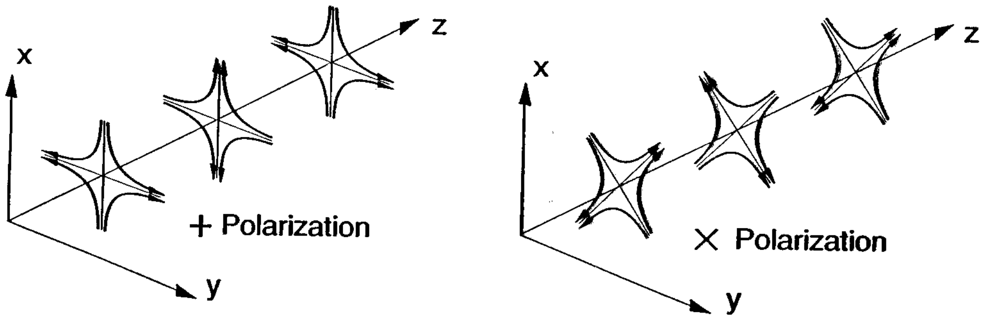
x
y
z
+ Polarization
x
y
z
× Polarization

Die in (23), (23a) und (23b) auftretenden Integrale, welche nichts anderes sind als zeitlich variable Trägheitsmomente, nennen wir im folgenden zur Abkürzung J_{22}, J_{33}, J_{23}. Dann ergibt sich für die Intensität $\mathfrak{f}_x$ der Energiestrahlung aus (18)

$$\mathfrak{f}_x = \frac{\varkappa}{64\pi^2 R^2}\left[\left(\frac{\partial^3 J_{22}}{\partial t^3}\right)^2 + 2\left(\frac{\partial^3 J_{23}}{\partial t^3}\right)^2 + \left(\frac{\partial^3 J_{33}}{\partial t^3}\right)^2\right]. \qquad (20)$$

SPHERICALLY SYMMETRIC MOTION RADIATES GRAVITATIONAL WAVES

1918 VI. VII. VIII

SITZUNGSBERICHTE

DER

KÖNIGLICH PREUSSISCHEN

AKADEMIE DER WISSENSCHAFTEN

BERLIN 1918

VERLAG DER KÖNIGLICHEN AKADEMIE DER WISSENSCHAFTEN

IN KOMMISSION BEI GEORG REIMER

Über Gravitationswellen.

Von A. Einstein.

(Vorgelegt am 31. Januar 1918 [s. oben S. 79].)

Die wichtige Frage, wie die Ausbreitung der Gravitationsfelder erfolgt, ist schon vor anderthalb Jahren in einer Akademiearbeit von mir behandelt worden[1]. Da aber meine damalige Darstellung des Gegenstandes nicht genügend durchsichtig und außerdem durch einen bedauerlichen Rechenfehler verunstaltet ist, muß ich hier nochmals auf die Angelegenheit zurückkommen.

Wie damals beschränke ich mich auch hier auf den Fall, daß das betrachtete zeiträumliche Kontinuum sich von einem »galileischen« nur sehr wenig unterscheidet. Um für alle Indizes

$$g_{\mu\nu} = -\delta_{\mu\nu} + \gamma_{\mu\nu} \qquad (1)$$

Sind die Bedingungen (15) erfüllt, so stellt (14) eine mögliche Gravitationswelle dar. Um deren physikalische Natur genauer zu durchschauen, berechnen wir deren Dichte des Energiestromes $\frac{t_{41}}{i}$. Durch Einsetzen der in (15) gegebenen $\gamma'_{\mu\nu}$ in Gleichung (9) erhält man

$$\frac{t_{41}}{i} = \frac{1}{4\varkappa} f'^2 \left[\left(\frac{\alpha_{22} - \alpha_{33}}{2} \right)^2 + \alpha_{23}^2 \right]. \qquad (16)$$

$$\mathfrak{J}_{\mu\nu} = \int x_\mu x_\nu \rho \, dV_0 \tag{23}$$

gesetzt; $\mathfrak{J}_{\mu\nu}$ sind die Komponenten des (zeitlich variabeln) Trägheitsmomentes des materiellen Systems.

Auf analogem Wege erhält man

$$\int (T_{22} - T_{33}) \, dV_0 = \frac{1}{2} (\ddot{\mathfrak{J}}_{22} - \ddot{\mathfrak{J}}_{33}) . \tag{24}$$

Aus (7a) ergibt sich auf Grund von (22) und (24)

$$\gamma'_{23} = - \frac{\varkappa}{4 \pi R} \ddot{\mathfrak{J}}_{23} . \tag{25}$$

$$\frac{\gamma'_{22} - \gamma'_{33}}{2} = - \frac{\varkappa}{4 \pi R} \left(\frac{\ddot{\mathfrak{J}}_{22} - \ddot{\mathfrak{J}}_{33}}{2} \right) . \tag{26}$$

Die $\mathfrak{J}_{\mu\nu}$ sind nach (7a), (22), (24) für die Zeit $t - R$ zu nehmen, also Funktionen von $t - R$, oder bei großem R in der Nähe der x-Achse auch Funktionen von $t - x$. (25), (26) stellen also Gravitationswellen dar, deren Energiefluß längs der x-Achse gemäß (16) die Dichte

$$\frac{t_{41}}{i} = \frac{\varkappa}{64 \pi^2 R^2} \left[\left(\frac{\dddot{\mathfrak{J}}_{22} - \dddot{\mathfrak{J}}_{33}}{2} \right)^2 + \dddot{\mathfrak{J}}_{23}^{\,2} \right] \tag{27}$$

besitzt.

THE QUADRUPOLE FORMULA A FACTOR OF 2 TOO SMALL

Physics of gravitational wave detection in addition to gravitation itself

- Quantum mechanics of the electromagnetic radiation field
  - Phase noise
  - Radiation pressure noise
  - Squeezed light
  - Control of scattering and diffraction
- Low dissipation mechanical systems
  - Fluctuation-dissipation theorem
  - Noise free damping systems
- Vibration isolation and inertial sensing systems
  - Inertial references
  - Servo control systems
  - Digital filtering
- Techniques to evaulate and circumvent random noise

Technical advances and experimental and observational elegance bring reality to the field and are interesting to students
DO NOT FORGET THEM IN YOUR COURSES

- Direct detection of gravitational waves
  - Strong field gravitation
  - Wave kinematics
  - Inventory of the universe
  - Measurement of a gravitational collapse
  - Neutron star equation of state
- Indirect detection of gravitational waves – CMB measurements
  - Polarization: primeval GW and inflation
  - Spectral index of the fluctuations
  - Lensing conversion E to B
- Direct measurement of frame dragging
- High precision weak principle of equivalence test
- Second order redshift with trapped atom clocks
- Bending of light to second order:stellar interferometry
- Strong principle of equivalence tests: clocks in different potentials
- Search for scalar fields in gravitation
- What is the dark matter
- What is the nature of the dark energy